




Thermal evaluation of a heat pipe working with *n*-pentane-acetone and *n*-pentane-methanol binary mixtures

M. M. Sarafraz¹ · Zhe Tian² · I. Tlili³ · Sabeena Kazi⁴ · Marjan Goodarzi⁵ 

Received: 3 April 2019 / Accepted: 24 May 2019 / Published online: 1 June 2019
© Akadémiai Kiadó, Budapest, Hungary 2019

Abstract

In the present study, a set of experiments were accomplished to appraise the thermal performance and heat transfer of *n*-pentane-acetone and *n*-pentane-methanol mixtures inside a gravity-assisted thermosyphon heat pipe. Pure *n*-pentane, acetone and methanol were also tested as the carrying fluid to produce some reference data. The heat pipe was manufactured from copper with length and diameter of 290 and 20 mm, respectively. The effect of multiple factors covering the input heat to the evaporator section, the filling ratio of the carrying fluid, heat pipe tilt angle and also the type of the carrying fluid on temperature distribution and thermal performance of the heat pipe was investigated. The results demonstrated that the thermo-physical properties of the carrying fluid were the key factor controlling the heat pipe efficiency. The vapour pressure and boiling temperature of the carrying fluid controlled the thermal efficiency of the system such that for *n*-pentane-acetone, the highest thermal efficiency was obtained. Also, it was identified that the filling ratio of the system is a key operating factor such that the value of the filling ratio was small for the evaporative carrying fluid (binary mixtures), while it was large for the non-evaporative carrying fluids. Also, heat pipe tilt angle was impressed by the type of the carrying fluid; the optimum tilt angle was 55 degree for the binary mixtures, while it was 65° for the pure liquids.

Keywords *n*-pentane · Acetone · Methanol · Heat pipe · Thermal performance · Gravity-assisted

Introduction

Efficient cooling of the high-temperature systems is one of the main targets in thermal engineering. Also, cooling systems with the capability to remove heat from high heat flux surface are demanded in various industrial and domestic sectors [1–6]. Generally, a thermal process under high heat flux (e.g. 60 kW m⁻² [7]) needs a cooling system, with the capability to operate at two-phase flow conditions [6, 8–11]. This is owing to the forming of nucleate boiling phenomenon on the heating surface. Boiling phenomenon is considered as a complicated heat transfer with wide usages in boilers, power cycles, reactors and automotive cooling loops [12–24]. The heat transfer coefficient in boiling systems is relatively larger than the single-phase heat transfer systems owing to the bubble interaction, the evaporation mechanism together with the convective heat transfer [25–33]. Therefore, extensive research has been devoted to utilise the boiling heat transfer mechanism in various cooling systems with the

✉ Marjan Goodarzi
marjan.goodarzi@tdtu.edu.vn

¹ School of Mechanical Engineering, The University of Adelaide, South Australia, Australia

² School of Engineering, Ocean University of China, Qingdao 266100, China

³ Department of Mechanical and Industrial Engineering, College of Engineering, Majmaah University, Al-Majmaah 11952, Saudi Arabia

⁴ Department of Computer Science, College of Computer and Information Sciences, Majmaah University, Al-Majmaah 11952, Saudi Arabia

⁵ Sustainable Management of Natural Resources and Environment Research Group, Faculty of Environment and Labour Safety, Ton Duc Thang University, Ho Chi Minh City, Vietnam

view of taking benefits from great heat transfer coefficient [25–30, 32–37]. Also, many resources were dedicated to find a suitable carrying fluid for cooling systems. Pure and binary mixtures and even the liquid metals are examples of such efforts [38–40].

Heat pipes are categorised in the group of passive devices [41–43] without the need for external energy (e.g. membranes [44]) working under two-phase flow regime [45–50], which enables one to transfer high heat values within a confined zone [51–57]. Heat pipes can have various applications in solar systems [58–60] and microelectronic cooling systems [61–63]. A heat pipe does not need any external energy for the heat transfer, and as a result, the heat pipe performance is severely related to the heat transfer specifications of the carrying fluid inside the device [64–67]. Each heat pipe includes three major parts including the evaporator, the adiabatic and the condenser sections. The evaporator section absorbs the heat in which this heat is transported to the carrying fluid. The carrying fluid is evaporated and transferred via the adiabatic region to the condenser section, in which the absorbed thermal energy is delivered to the atmosphere. Thus, the thermal efficiency of the evaporator and also the condenser section are two key parameters influencing the heat pipe efficiency. At high heat fluxes, in the evaporator section, the nucleate pool boiling heat transfer is responsible for the evaporation of the carrying fluid, which has extensively been studied in the literature [68–81].

To enhance the thermal efficiency of the heat pipes, much effort has been made to identify new approaches to utilise the passive techniques for enhancing the heat transfer coefficient of the evaporator. Nanofluid is one of the potential options as a carrying fluid, and much effort has been made to find some applications for this wonderful material [5, 82–85]. For example, Dehaj et al. [86] performed a series of experimental tests to assess the thermal efficiency of a heat pipe filled with MgO/water nanofluid. The results revealed that the performance of the heat pipe was enhanced by utilising the nanofluid in the heat pipe. Also, adding more nanoparticles to the carrying fluid further enhanced the heat transfer coefficient and efficiency of the heat pipe. Senthilkumar et al. [3] experimentally assessed the efficiency of a heat pipe filled with H₂O and nanofluid. They found out that the heat pipe efficiency strongly corresponds to the filling ratio, heat transfer characteristics of the carrying fluid and the performance of the evaporator. Xu et al. [87] assessed the efficiency of a heat pipe with zeotropic binary mixtures and implemented deionised water mixed with HFE-7100. They found that for the high heat fluxes, the mixture can potentially reduce the thermal resistance of the heat pipe and improve the thermal efficiency of the system. It was also identified that the boiling heat transfer is the mechanism of heat transfer in

the evaporator. However, dry-out restricts the heat transfer of the system.

Zhang et al. [88] introduced a novel heat pipe for cooling the high heat flux systems. The efficiency of the heat pipe was assessed via a set of experiments, and it was found that the structure of the wick, temperature distribution and also the thermal resistance of the heat pipe are key parameters that affect the efficiency of the heat pipe. Sarafraz et al. [70] carried out some experiments to evaluate the heat transfer specifications of various carrying fluids including ethylene glycol, water and also two nanofluids inside a straight heat pipe. The efficacy of various working conditions on the thermal efficiency of the system was evaluated, and it was revealed that the heat transfer coefficient of the heat pipe notably increased, when nanofluids were utilised as the carrying fluid inside heat pipe. Also, they demonstrated that the filling ratio and also heat pipe tilt angle were two crucial parameters, which were optimised for the test heat pipe. In another investigation, Sarafraz et al. [89] perused the potential efficacy of the fouling formation of the particles inside a straight heat pipe fabricated from copper. They noticed that over a transient study, the particles deposited inside the evaporator and caused the heat pipe to be failed. However, for a period of operation, the thermal efficiency of the heat pipe was considerably improved. So, the operation of the heat pipe was categorised into two stages of operation with a clean evaporator and operation with the evaporator with fouling. Therefore, they developed a new formula to forecast the fouling formation inside the heat pipe. Qu et al. [90] demonstrated a new type of the heat pipe with the potential application in electric vehicles. H₂O, C₂H₅OH and binary fluid mixtures of them at various compositions were tested inside the heat pipe, and it was found that for the developed heat pipe, the temperature distribution was uniform and the efficiency of the heat pipe for cooling the batteries was satisfactory with binary mixtures of water–ethanol.

Facing the above literature, heat pipes can have a bright future in thermal engineering providing that more research is conducted to identify new carrying fluids with plausible heat transfer characteristics to further enhance the efficacy of the system. Therefore, in the present perusal, the thermal efficiency of a straight gravity-assisted heat pipe is evaluated for various carrying fluids including, *n*-pentane-methanol, *n*-pentane-acetone, pure *n*-pentane, acetone and methanol. Binary mixtures have been found to represent a relatively plausible heat and mass transfer in single- and two-phase heat and mass transfer regimes [12, 40, 78, 79, 81, 91–99]. Efficacy of various factors including the exerted heat flux, the filling ratio and the tilt angle values on the thermal performance of the thermal system was experimentally considered and discussed.

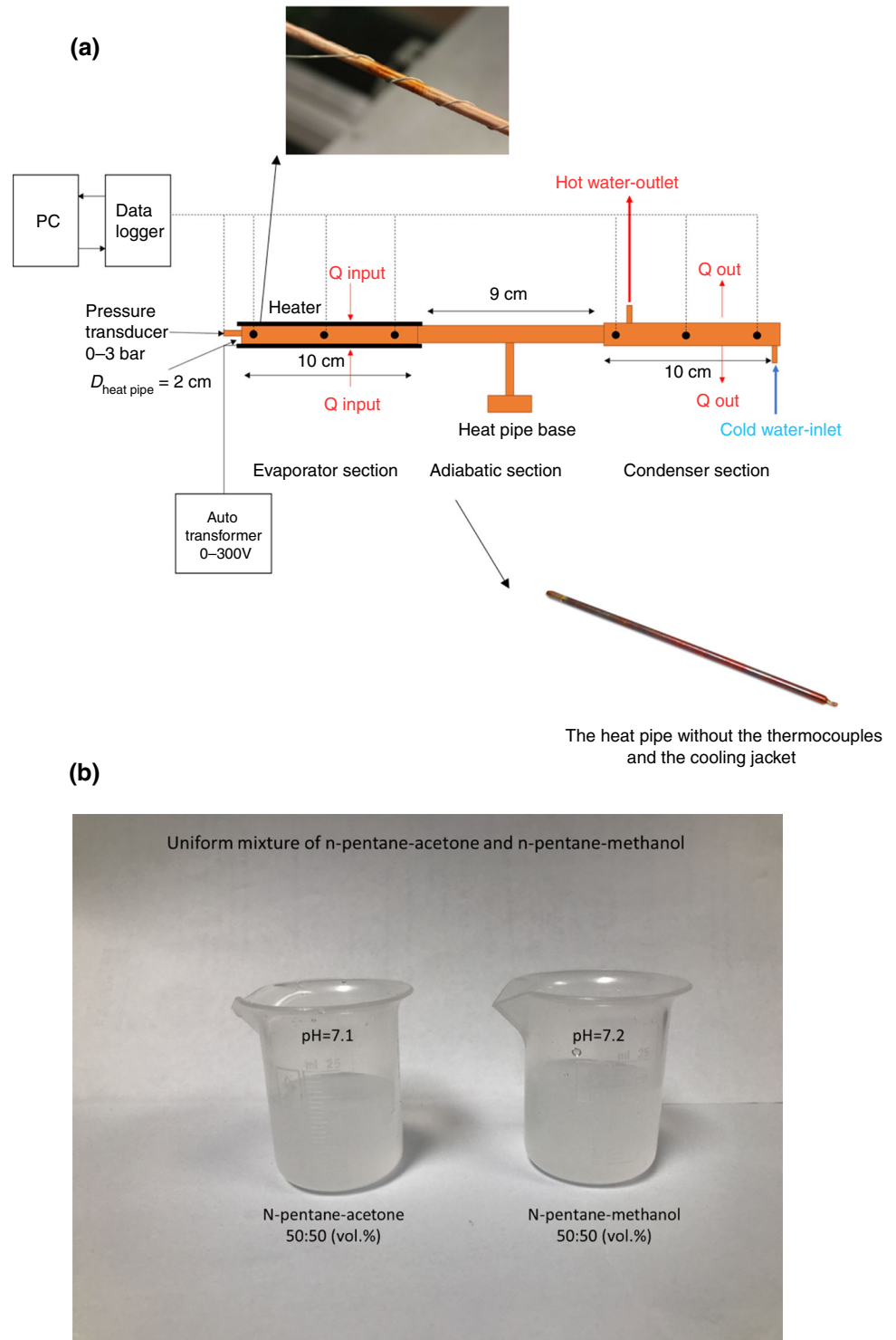
Experimental

Test rig

Figure 1 illustrates the schematic of the employed apparatus in the present study. The test rig includes the heat

pipe, which is heated up with a flexible cartridge heater (1000 W), adiabatic section and also a condenser which is constantly cooled with a cooling jacket conjunct to a thermostat bath. The flow rate of the thermostat bath was controlled such that a constant temperature of 20 °C was maintained in the condenser section. This provided a

Fig. 1 **a** A schematic of the utilised apparatus and **b** the prepared mixtures



condition to perform a back-to-back comparison between the results of the experiments. For measuring the temperature profile of the heat pipe, eight k-type thermocouples (three for the evaporator, two for the adiabatic and three for the condenser) were employed. The thermocouples were installed on the surface of the heat pipe. To minimise the thermal resistance between the thermocouples and the body of heat pipe, silicone paste (grade A with thermal conductivity of 4.5 W (mK)^{-1}) was employed. The thermocouples were connected to a data logger with data reading frequency of 1 kHz. Notably, the flexible cartridge heater was connected to an AC autotransformer (0–300 V) to provide the necessary heat for the heater. Also, a pressure transducer was employed to control the internal pressure of the heat pipe to warrant that the heat pipe is not pressurised at high heat flux conditions. To change the heat pipe tilt angle, a portable inclinometer was installed on the top of the heat pipe, while a base was designed such that the tilt angle of heat pipe could be changed from 0° to 85° . Also, to change the filling ratio of the heat pipe, the carrying fluid was charged into the heat pipe using a syringe pump. During the charging process, a vacuum pump was employed. Hence, the direct contact between air and *n*-pentane or methanol was prevented. This led the experiments to be conducted in a safe environment. The syringe pump provided conditions to accurately fill the heat pipe with various carrying fluids. Also, the internal wall of the heat pipe was sandblasted so the roughness of the surface of the evaporator was sufficient to handle the boiling mechanism.

To prepare the carrying fluids, *n*-pentane, acetone and methanol were purchased from Sigma-Aldrich and the binary mixtures were prepared at 50:50 (by volume fraction) of *n*-pentane and acetone, and *n*-pentane and methanol. The pH of the mixture was controlled to ensure that a two-phase mixture is not formed and also the carrying fluid is not corrosive to damage the evaporator section. This is because the corrosion of copper is very sensitive to the pH value of the liquids. Hence, the pH value was set at ~ 7 employing a buffer solution of NaOH and HCl at 0.1 mM.

Experimental procedure

To perform the experiments, first, heat pipe was heated up and the ventilation valve was opened to de-gas the heat pipe, while using the syringe pump, the heat pipe was charged with the carrying fluid. Then, the evaporator section was heated up and system was allowed to reach a thermal equilibrium; then, the temperatures were recorded. The same approach was applied for all the sensitivity analysis and experimental stages. Experimental tests were accomplished three times to assure the reproducibility and

repeatability of the outcomes. The thermocouples were also calibrated for deionised water to warrant the accuracy of the temperature reading. Also, the pressure sensor was calibrated for water as well to ensure about the uncertainty values claimed by the manufacturer.

Data reduction and uncertainty analysis

To estimate the thermal resistance of the studied thermal system, Eq. (1) has been employed [100]:

$$R = \frac{T_e - T_c}{Q_e} \quad (1)$$

In the above equation, T_c is the condenser and T_e is the evaporator temperature. Likewise, Q_e is the total thermal energy applied to the evaporator section of the heat pipe, which can be calculated by measuring the voltage and current of the flexible cartridge heater as follows:

$$Q_e = V \times I \quad (2)$$

To assess the thermal efficiency of the thermal system, the heat transfer coefficient of the evaporator was measured at various working conditions using the following equation:

$$q_e'' = \frac{Q_e}{\pi \times D \times L} \quad (3)$$

where

$$h_e = \frac{q_e''}{\Delta T} \quad (4)$$

In Eq. (3), D is the diameter of the evaporator which equals to the diameter of the heat pipe as well, L is the length of the heat pipe. Using Eq. (3), the heat transfer coefficient of the evaporator was calculated with Eq. (4) in which q_e'' is the exerted heat flux to the evaporator and ΔT is the temperature difference. Heat flux is also determined as the ratio of the exerted heat to area of the evaporator. To estimate the potential uncertainty of the instruments and also the experiments, the Moffat method was utilised [101]. Also, to compute the heat loss from the body of the heat pipe, an energy balance was applied to the evaporator and the condenser. Figure 2 represents the outcomes of the energy balance for the applied heat to the evaporator and that of released in the condenser. The variation between the heat input and output is the heat loss, which revealed a 7.9% heat loss despite a heavy insulation employed for the adiabatic and the evaporator sections.

Table 1 exhibits the uncertainties of the instruments and also the measured parameters in the experiments.

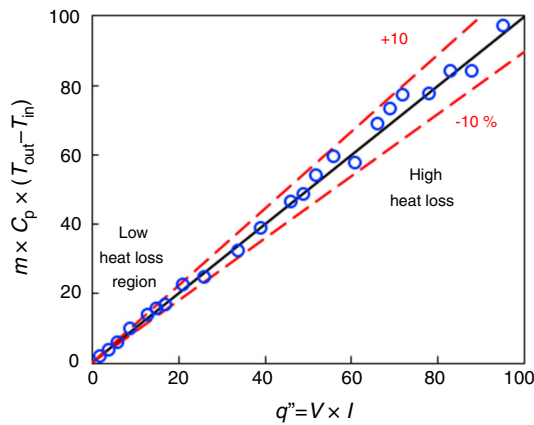


Fig. 2 Heat loss analysis between the condenser and the evaporator sections

Results and discussion

Heat flux to evaporator

Figure 3 illustrates the alteration of the temperature with the length of the system for different carrying fluids at heat input of 100 W. It is clear that the temperature is the highest in the evaporator, while it diminishes along the length of the heat pipe. In the adiabatic section, the temperature is almost constant since this part is heavily insulated and also there is no input or output heat to change the temperature distribution. Amongst the carrying fluids used inside the heat pipe, *n*-pentane-acetone showed the highest thermal performance and temperature profile distribution, followed by *n*-pentane-methanol, pure *n*-pentane, acetone and methanol. For example, in the evaporator section, for a specific heat input of 100 W, the evaporator temperature is 68 °C, 65 °C, 62 °C, 60 °C and 58 °C for *n*-pentane-acetone, *n*-pentane-methanol, pure *n*-pentane, acetone and methanol, respectively. As can also be seen, the temperature distribution for *n*-pentane-acetone is the uppermost; showing that the heat transfer specifications of the mixture

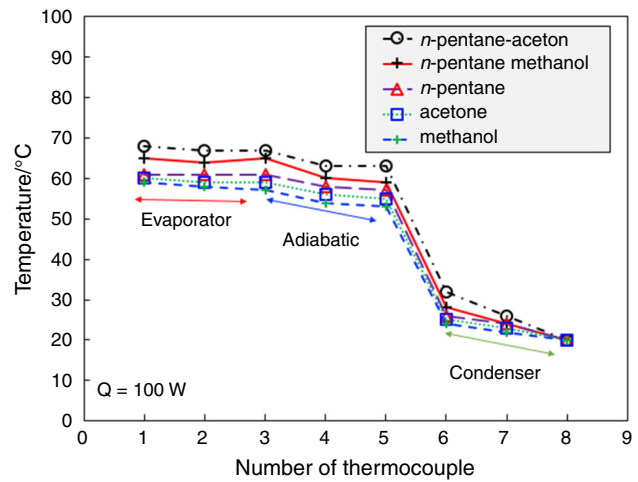


Fig. 3 Alteration of the temperature with the length of the heat pipe at filling ratio of 0.2 and tilt angle of 5 degree

are plausible such that the thermal resistance is minimised. This can be ascribed to the heat transfer mechanism within the evaporator. As the boiling temperature of acetone and *n*-pentane is 56 °C and 36.1 °C, respectively, the nucleate boiling is the predominant heat transfer mechanism within the heat pipe. As discussed before, the nucleate boiling has a larger heat transfer coefficient in comparison with convective mechanism. This enlargement can be attributed to the formation of the bubbles inside the evaporator and also the interaction between the bubbles on the surface, which facilitates the heat transfer from the evaporator walls to the carrying fluid owing to the micro-convective streams around the bubbles.

Thermal resistance

To further analysis the efficacy of the carrying fluid on the temperature profile of the system, the thermal resistance of the heat pipe was checked against a wide range of the heat fluxes. Figure 4 demonstrates the alteration of the thermal

Table 1 Uncertainty values of the used instruments and the parameters

Instrument/parameter	Manufacturer	Uncertainty value
Instruments		
Temperature	Omega	± 0.5 K
Pressure	Fluke	1%
Inclination of the heat pipe	Europac	0.5%
Voltage of the heater	Omega multi-meter	0.1%
Current of the heater	Omega multi-meter	0.1%
Syringe pump	Techno-motor CO.	1%
Parameters		
Heat transfer coefficient	–	7.1%
Filing ratio	–	0.6% (max.)
Tilt angle	–	1% (max.)

resistance of the heat pipe for various carrying fluids. It is clear that the thermal resistance parameter diminished asymptotically with the heat flux increment. For example, for pure acetone, at q'' of 25 kW m^{-2} , the thermal resistance is $0.7 \text{ m}^2 \text{ K kW}^{-1}$, while it is $0.23 \text{ m}^2 \text{ K kW}^{-1}$ for the exerted heat flux (q'') of 90 kW m^{-2} . Also, it is obvious that *n*-pentane-acetone mixture has the lowest thermal resistance, followed by *n*-pentane methanol mixture. However, for the pure carrying fluids including *n*-pentane, acetone and methanol, the thermal resistance is highest for methanol and lowest for *n*-pentane. A rough comparison between the thermal resistance of the system for binary mixtures and the pure liquids showed that for binary mixtures, system represented lower thermal resistance value. This can be attributed to the mixture effect occurring in binary *n*-pentane-acetone and *n*-pentane-methanol solutions, which in turn promotes the thermal characteristics of the mixtures involving thermal conductivity and the heat capacity. For example, for *n*-pentane-acetone at q'' of 90 kW m^{-2} , the thermal resistance is $0.17 \text{ m}^2 \text{ K kW}^{-1}$, while it is $0.19 \text{ m}^2 \text{ K kW}^{-1}$, $0.21 \text{ m}^2 \text{ K kW}^{-1}$, $0.23 \text{ m}^2 \text{ K kW}^{-1}$ and $0.25 \text{ m}^2 \text{ K kW}^{-1}$ for *n*-pentane-methanol, *n*-pentane, acetone and methanol, respectively. Hence, binary mixtures of *n*-pentane seem to have more plausible heat transfer characteristics in comparison with pure carrying fluids.

Heat transfer coefficient

Figure 5 illustrates the dependency of the HTC of the evaporator on the exerted heat flux and for studied carrying fluids. As evidenced, for heat fluxes $< 25 \text{ kW m}^{-2}$, the heat transfer coefficient changes slightly for all the carrying fluids and within this range, the heat transfer coefficient

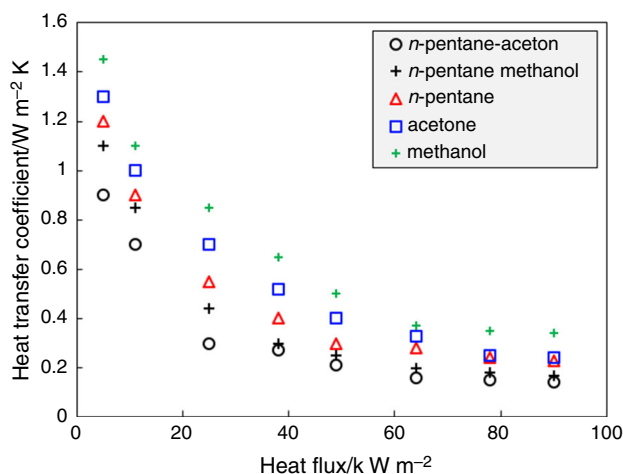


Fig. 4 Variation in the thermal resistance of the system with the exerted heat flux to the evaporator at filling ratio of 0.2 and tilt angle of 5 degree

slightly reduces, with any decrease in the q'' . However, for larger heat fluxes, the trends change such that the *n*-pentane-acetone mixture has the largest heat transfer coefficient, followed by *n*-pentane-methanol. For example, for *n*-pentane-acetone, at q'' of 11 kW m^{-2} , the heat transfer coefficient is $1190 \text{ W m}^{-2} \text{ K}$, while it is 7058 kW m^{-2} , 6870 kW m^{-2} , 6430 kW m^{-2} and 5988 kW m^{-2} for *n*-pentane-methanol, pure *n*-pentane, pure acetone and pure methanol. This may be referred to the high vapour pressure of the *n*-pentane, acetone and methanol, which in turn facilitates the incipience of boiling mechanism. It also promotes the bubbles formation inside the evaporator as well, which further enhances the heat transfer coefficient of the evaporator. Also, the size of the bubbles is strongly related to the surface tension and density of the vapour and liquid. Thereby, for *n*-pentane and acetone mixture, due to the small surface tension, it is expected that the bubbles become smaller and as a result, bubble jets are formed and intensify the heat transfer coefficient. This requires further investigation that is above the targets of the present study.

Filling ratio

Filling ratio is determined as the ratio of the volume of the carrying fluid to the total volume of the evaporator [102]. Figure 6 exhibits the alteration of the heat transfer coefficient with the filling ratio value for various carrying fluids at $q'' = 90 \text{ kW m}^{-2}$. For *n*-pentane-acetone, as can be seen in Fig. 6, at filling ratio of 0.4, the heat transfer coefficient reaches the highest value of $\sim 8500 \text{ W m}^{-2} \text{ K}$. This is because *n*-pentane-acetone is an evaporative mixture and its vapour can easily fill the heat pipe volume. Also, the trend between the value of the liquid inside the heat pipe and the available space for the vapour to be transported from the evaporator to the condenser can be considered as a

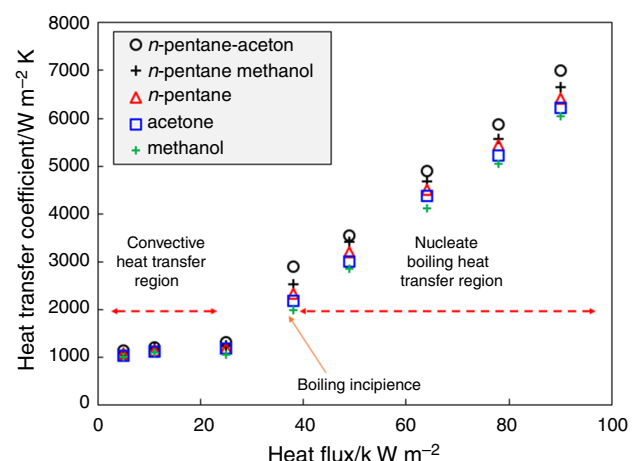


Fig. 5 Alteration of the heat transfer coefficient with the exerted heat flux at filling ratio of 0.2 and tilt angle of 5 degree

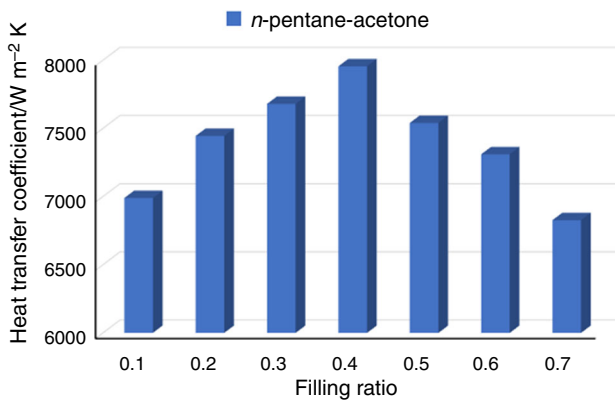


Fig. 6 Heat transfer coefficient versus the filling ratio for *n*-pentane-acetone mixture

trade-off. Thereby, the amount of the liquid becomes a limiting parameter. Hence, the heat pipe performance severely depends on the filling ratio. Therefore, there is an optimum point in which the thermal performance of the heat pipe is maximised which is 0.4 for *n*-pentane-acetone and it can be different for other carrying fluids and for other heat pipes with different geometrical specifications.

As is clear in Fig. 7, the heat transfer coefficient of the heat pipe for *n*-pentane-methanol increases up to $7710 W m^{-2} K$ at filling ratio of 0.5 and then decreases. This can be attributed to the fact that *n*-pentane-methanol is less evaporative than *n*-pentane-acetone; hence, more liquid may be charged into the heat pipe, and the optimum filling ratio is 0.5.

Figure 8 also represents the alteration of the heat transfer coefficient with the filling ratio parameter for pure *n*-pentane, acetone and methanol. As can be seen, for all of them, the filling ratio is 0.65, which is completely owing to the large vapour pressure of the carrying fluids. Hence, a large portion of the carrying fluid remains liquid inside the evaporator which limits the available space for the vapour phase inside the heat pipe. Also, as is evident, *n*-pentane

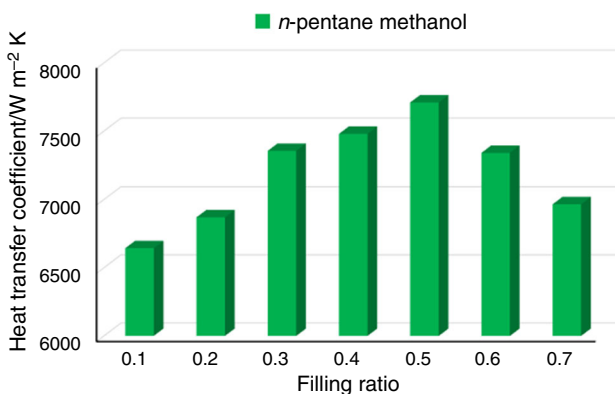


Fig. 7 Heat transfer coefficient versus the filling ratio for *n*-pentane-methanol mixture

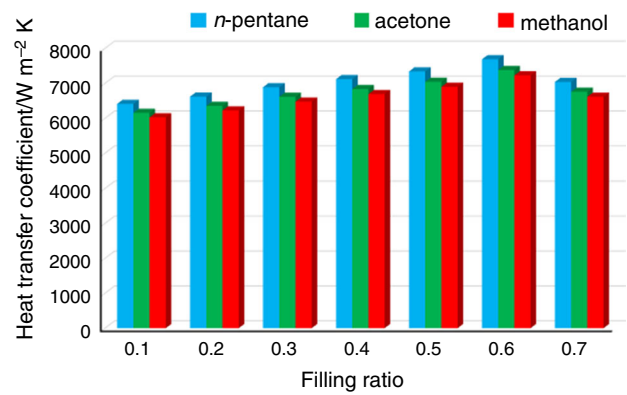


Fig. 8 Heat transfer coefficient versus the filling ratio for *n*-pentane, acetone and methanol at $90 kW m^{-2}$ and tilt angle of 5 degree

has the largest heat transfer coefficient followed by acetone and methanol. Also, the optimum value of the filling ratio was 0.6, wherein the heat transfer coefficient of the heat pipe was maximised ($6200 W m^{-2} K$, $6080 W m^{-2} K$ and $5900 W m^{-2} K$ for *n*-pentane, acetone and methanol, respectively).

Tilt angle

Figure 9 represents the alteration of the heat transfer coefficient with the tilt angle of the heat pipe for studied carrying fluids. Clearly, the optimum tilt angle is different for the mixtures and the pure liquids and it is 55° for the mixtures and 65° for the pure liquids. This is because the liquid in the condenser is returning to the evaporator using gravity-assisted falling film. For mixtures, most of the liquid is evaporated; hence, the effect of the gravity is very small; however, for the pure liquid, the effect of the gravity is more pronounced as more liquid is available in the heat pipe. Therefore, the tilt angle is potentially larger than the binary test mixtures.

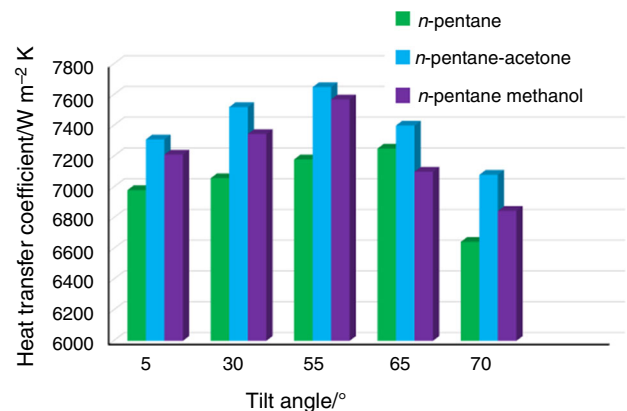


Fig. 9 Heat transfer coefficient versus tilt angle for various carrying fluids

It is worth saying that a collation between the obtained results and prior investigations reveals that the tilt angle and filling ratio are almost the same value as reported in the past. Also, the heat transfer coefficient is within the range of HTC already introduced in the prior studies [70, 96, 103] within $\pm 10\%$ deviation.

Conclusions

An experimental study was accomplished to evaluate the thermal performance of *n*-pentane-acetone and *n*-pentane-methanol mixtures together with pure *n*-pentane, acetone and methanol. It was identified that *n*-pentane was found to be the most promising carrying fluid for the gravity-assisted heat pipe. Also, the heat pipe was assessed for various working conditions and the following conclusions were drawn:

- It was revealed that with an enhancement in the exerted heat flux, the performance of the heat pipe was augmented due to the conversion of the heat transfer mechanism; from convection heat transfer to nucleate boiling. The presence of the bubbles further intensified the heat transfer mechanism in the evaporator owing to the agitation of the liquid close to the internal wall of the evaporator and also the micro-convective streams formed inside the evaporator.
- It was also identified that the vapour pressure of the carrying fluid can be a key parameter such that for the evaporative mixtures such as *n*-pentane-acetone, the heat transfer coefficient was larger than *n*-pentane-methanol and the pure liquids.
- Filling ratio was also a key factor which mutates the efficiency of the heat pipe. For the evaporative mixture such as *n*-pentane-acetone, a large portion of the carrying fluid was evaporated; hence, a trade-off trend was identified between the extant region inside the heat pipe and the amount of the vapour such that the transportation of the vapour from the evaporator to the condenser was limited to the available space inside the heat pipe. Therefore, the filling ratio value for the evaporative mixtures was 0.4 and 0.5 for *n*-pentane-acetone and *n*-pentane-methanol, respectively.
- Tilt angle was another key parameter that alters the thermal efficiency of the system. This is because the higher the tilt angle, the larger the gravity effect. Hence, pure liquids require larger tilt angle to facilitate the return of the carrying fluid to the evaporator from the condenser section. However, the mixtures required small tilt angle as small amount of the mixtures was in the liquid phase.

Acknowledgements First author of this work tends to appreciate Rayan Sanat Co. for sharing their facilities. Dr. Zhe Tian acknowledges the NSFC (51709244), Taishan Scholar (tsqn201812025) and Fundamental Research for Central Universities (201941008). Dr. Sabeena Kazi would like to thank Deanship of Scientific Research at Majmaah University for supporting this work under the Project Number No. 1440-107.

Compliance with ethical standards

Conflict of interest The authors of the present work declare no conflict of interest.

References

1. Mudawar I. Assessment of high-heat-flux thermal management schemes. *IEEE Trans Compon Packag Technol.* 2001;24:122–41.
2. Agostini B, Fabbri M, Park JE, Wojtan L, Thome JR, Michel B. State of the art of high heat flux cooling technologies. *Heat Transfer Eng.* 2007;28:258–81.
3. Senthilkumar R, Vaidyanathan S, Sivaraman B. Effect of inclination angle in heat pipe performance using copper nanofluid. *Procedia Eng.* 2012;38:3715–21.
4. Ali H, Kamran M, Ali H, Imran S. Condensation heat transfer enhancement using steam-ethanol mixtures on horizontal finned tube. *Int J Therm Sci.* 2019;140:87–95.
5. Sajid MU, Ali HM. Recent advances in application of nanofluids in heat transfer devices: a critical review. *Renew Sustain Energy Rev.* 2019;103:556–92.
6. Khattak Z, Ali HM. Air cooled heat sink geometries subjected to forced flow: a critical review. *Int J Heat Mass Transf.* 2019;130:141–61.
7. Lee J, Mudawar I. Two-phase flow in high-heat-flux micro-channel heat sink for refrigeration cooling applications: part I—pressure drop characteristics. *Int J Heat Mass Transf.* 2005;48:928–40.
8. Ali HM, Saieed A, Pao W, Ali M. Copper foam/PCMs based heat sinks: an experimental study for electronic cooling systems. *Int J Heat Mass Transf.* 2018;127:381–93.
9. Usman H, Ali HM, Arshad A, Ashraf MJ, Khushnood S, Janjua MM, Kazi SN. An experimental study of PCM based finned and un-finned heat sinks for passive cooling of electronics. *Heat Mass Transf.* 2018;54:3587–98.
10. Arshad A, Ali HM, Yan W-M, Hussein AK, Ahmadlouydarab M. An experimental study of enhanced heat sinks for thermal management using n-eicosane as phase change material. *Appl Therm Eng.* 2018;132:52–66.
11. Safdari Shadloo M. Numerical simulation of compressible flows by lattice Boltzmann method. *Numer Heat Transf Part A Appl.* 2019;75:167–82.
12. Sarafraz MM. Nucleate pool boiling of aqueous solution of citric acid on a smoothed horizontal cylinder. *Heat Mass Transf.* 2012;48:611–9.
13. Arya A, Sarafraz M, Shahmiri S, Madani S, Nikkhah V, Nakhjavani S. Thermal performance analysis of a flat heat pipe working with carbon nanotube-water nanofluid for cooling of a high heat flux heater. *Heat Mass Transf.* 2018;54:985–97.
14. Nakhjavani M, Nikkhah V, Sarafraz M, Shoja S, Sarafraz M. Green synthesis of silver nanoparticles using green tea leaves: experimental study on the morphological, rheological and antibacterial behaviour. *Heat Mass Transf.* 2017;53:3201–9.

15. Nikkhhah V, Sarafraz M, Hormozi F. Application of spherical copper oxide (II) water nano-fluid as a potential coolant in a boiling annular heat exchanger. *Chem Biochem Eng Q*. 2015;29:405–15.
16. Salari E, Peyghambarzadeh M, Sarafraz MM, Hormozi F. Boiling heat transfer of alumina nano-fluids: role of nanoparticle deposition on the boiling heat transfer coefficient. *Periodica Polytech, Chem Eng*. 2016;60:252–8.
17. Salari E, Peyghambarzadeh S, Sarafraz M, Hormozi F, Nikkhhah V. Thermal behavior of aqueous iron oxide nano-fluid as a coolant on a flat disc heater under the pool boiling condition. *Heat Mass Transf*. 2017;53:265–75.
18. M. Sarafraz, Experimental investigation on pool boiling heat transfer to formic acid, propanol and 2-butanol pure liquids under the atmospheric pressure, (2013).
19. Sarafraz M, Arya A, Nikkhhah V, Hormozi F. Thermal performance and viscosity of biologically produced silver/coconut oil nanofluids. *Chem Biochem Eng Q*. 2017;30:489–500.
20. Sarafraz MM, Hormozi F, Peyghambarzadeh SM, Vaeli N. Upward flow boiling to DI-water and CuO nanofluids inside the concentric annuli. *J Appl Fluid Mech*. 2015;8:4.
21. Sarafraz M, Nikkhhah V, Madani S, Jafarian M, Hormozi F. Low-frequency vibration for fouling mitigation and intensification of thermal performance of a plate heat exchanger working with CuO/water nanofluid. *Appl Therm Eng*. 2017;121:388–99.
22. Sarafraz M, Nikkhhah V, Nakhjavani M, Arya A. Thermal performance of a heat sink microchannel working with biologically produced silver-water nanofluid: experimental assessment. *Exp Thermal Fluid Sci*. 2018;91:509–19.
23. Sarafraz M, Peyghambarzadeh S. Influence of thermodynamic models on the prediction of pool boiling heat transfer coefficient of dilute binary mixtures. *Int Commun Heat Mass Transfer*. 2012;39:1303–10.
24. Lebon B, Nguyen MQ, Peixinho J, Shadloo MS, Hadjadj A. A new mechanism for periodic bursting of the recirculation region in the flow through a sudden expansion in a circular pipe. *Phys Fluids*. 2018;30(3):031701.
25. Hopp-Hirschler M, Shadloo MS, Nieken U. A Smoothed Particle Hydrodynamics approach for thermo-capillary flows. *Comput Fluids*. 2018;176:1–19.
26. Jamalabadi MYA, DaqiqShirazi M, Kosar A, Shadloo MS. Effect of injection angle, density ratio, and viscosity on droplet formation in a microfluidic T-junction. *Theor Appl Mech Lett*. 2017;7:243–51.
27. Karimipour A, Bagherzadeh SA, Goodarzi M, Alnaqi AA, Bahiraei M, Safaei MR, Shadloo MS. Synthesized CuFe₂O₄/SiO₂ nanocomposites added to water/EG: evaluation of the thermophysical properties beside sensitivity analysis & EANN. *Int J Heat Mass Transf*. 2018;127:1169–79.
28. Karimipour A, D’Orazio A, Shadloo MS. The effects of different nano particles of Al₂O₃ and Ag on the MHD nano fluid flow and heat transfer in a microchannel including slip velocity and temperature jump. *Physica E*. 2017;86:146–53.
29. Nasiri H, Jamalabadi MYA, Sadeghi R, Safaei MR, Nguyen TK, Shadloo MS. A smoothed particle hydrodynamics approach for numerical simulation of nano-fluid flows. *J Therm Anal Calorim*. 2018;135(3):1–9.
30. Rashidi MM, Nasiri M, Shadloo MS, Yang Z. Entropy generation in a circular tube heat exchanger using nanofluids: effects of different modeling approaches. *Heat Transf Eng*. 2017;38:853–66.
31. Safaei M, Ahmadi G, Goodarzi M, Safdari Shadloo M, Goshayeshi H, Dahari M. Heat transfer and pressure drop in fully developed turbulent flows of graphene nanoplatelets–silver/water nanofluids. *Fluids*. 2016;1(3):20.
32. Safaei MR, Gooarzi M, Akbari OA, Shadloo MS, Dahari M. Performance evaluation of nanofluids in an inclined ribbed microchannel for electronic cooling applications. *Electron Cooling, InTech*. 2016.
33. Safaei MR, Safdari Shadloo M, Goodarzi MS, Hadjadj A, Goshayeshi HR, Afrand M, Kazi SN. A survey on experimental and numerical studies of convection heat transfer of nanofluids inside closed conduits. *Adv Mech Eng*. 2016;8(10):16878140 16673569.
34. Méndez M, Shadloo MS, Hadjadj A, Ducoin A. Boundary layer transition over a concave surface caused by centrifugal instabilities. *Comput Fluids*. 2018;171:135–53.
35. Shadloo MS, Hadjadj A, Bodony DJ, Hussain F, Lele SK Effects of heat transfer on transitional states of supersonic boundary layers. In: *Proceedings of the Summer Program*, 2016, pp. 175–184.
36. Shadloo M, Oger G, Le Touzé D. Smoothed particle hydrodynamics method for fluid flows, towards industrial applications: motivations, current state, and challenges. *Comput Fluids*. 2016;136:11–34.
37. Sharma S, Shadloo MS, Hadjadj A. Effect of thermo-mechanical non-equilibrium on the onset of transition in supersonic boundary layers. *Heat Mass Transf*. 2018. <https://doi.org/10.1007/s00231-018-2429-9>.
38. Sarafraz M, Arjomandi M. Demonstration of plausible application of gallium nano-suspension in microchannel solar thermal receiver: experimental assessment of thermo-hydraulic performance of microchannel. *Int Commun Heat Mass Transf*. 2018;94:39–46.
39. Sarafraz M, Arjomandi M. Thermal performance analysis of a microchannel heat sink cooling with Copper Oxide-Indium (CuO/In) nano-suspensions at high-temperatures. *Appl Therm Eng*. 2018;137:700–9.
40. Sarafraz M, Arya H, Arjomandi M. Thermal and hydraulic analysis of a rectangular microchannel with gallium-copper oxide nano-suspension. *J Mol Liq*. 2018;263:382–9.
41. Goshayeshi HR, Goodarzi M, Safaei MR, Dahari M. Experimental study on the effect of inclination angle on heat transfer enhancement of a ferrofluid in a closed loop oscillating heat pipe under magnetic field. *Exp Thermal Fluid Sci*. 2016;74:265–70.
42. Goshayeshi H, Goodarzi M, Dahari M. Effect of magnetic field on the heat transfer rate of kerosene/Fe₂O₃ nanofluid in a copper oscillating heat pipe. *Exp Thermal Fluid Sci*. 2015;68:663–8.
43. Goshayeshi HR, Safaei MR, Goodarzi M, Dahari M. Particle size and type effects on heat transfer enhancement of Ferro-nanofluids in a pulsating heat pipe. *Powder Technol*. 2016;301:1218–26.
44. Hopp-Hirschler M, Shadloo MS, Nieken U. Viscous fingering phenomena in the early stage of polymer membrane formation. *J Fluid Mech*. 2019;864:97–140.
45. Roghayeh A, Behshad GM, Omid S, Soteris M, Somchai K. Review on pulsating heat pipes: from solar to cryogenic applications. *Appl Energy*. 2018;222:475–84.
46. Esfahani JA, Safaiyan S, Rashidi S. Heat transfer in an eight-pass oscillating loop heat pipe equipped with cooling tower. *J Therm Anal Calorim*. 2018. <https://doi.org/10.1007/s10973-018-7835-1>.
47. Heydarian R, Shafii MB, Shirin-Abadi AR, Ghasempour R, Nazari MA. Experimental investigation of paraffin nano-encapsulated phase change material on heat transfer enhancement of pulsating heat pipe. *J Therm Anal Calorim*. 2019. <https://doi.org/10.1007/s10973-019-08062-6>.
48. Kumaresan G, Vijayakumar P, Ravikumar M, Kamatchi R, Selvakumar P. Experimental study on effect of wick structures on thermal performance enhancement of cylindrical heat pipes.

- J Therm Anal Calorim. 2018. <https://doi.org/10.1007/s10973-018-7842-2>.
49. Stephen EN, Asirvatham LG, Kandasamy R, Solomon B, Kondru GS. Heat transfer performance of a compact loop heat pipe with alumina and silver nanofluid. *J Therm Anal Calorim.* 2018. <https://doi.org/10.1007/s10973-018-7739-0>.
 50. Cacia K, Buitrago-Sierra R, Herrera B, Pabón E, Murshed SS. Nanofluids' stability effects on the thermal performance of heat pipes. *J Therm Anal Calorim.* 2018. <https://doi.org/10.1007/s10973-018-7787-5>.
 51. Dunn P, Reay DA. *Heat pipes.* Elsevier, 2012.
 52. Petukhov B. Heat transfer and friction in turbulent pipe flow with variable physical properties. *Adv Heat Transf.* 1970;6:503–64.
 53. Stephan P, Busse C. Analysis of the heat transfer coefficient of grooved heat pipe evaporator walls. *Int J Heat Mass Transf.* 1992;35:383–91.
 54. Udell KS. Heat transfer in porous media considering phase change and capillarity—the heat pipe effect. *Int J Heat Mass Transf.* 1985;28:485–95.
 55. Zhang Y, Faghri A. Heat transfer in a pulsating heat pipe with open end. *Int J Heat Mass Transf.* 2002;45:755–64.
 56. Shafii M, Faghri A, Zhang Y. Analysis of heat transfer in unlooped and looped pulsating heat pipes. *Int J Numer Meth Heat Fluid Flow.* 2002;12:585–609.
 57. Liu Z-H, Xiong J-G, Bao R. Boiling heat transfer characteristics of nanofluids in a flat heat pipe evaporator with micro-grooved heating surface. *Int J Multiph Flow.* 2007;33:1284–95.
 58. Sabiha M, Saidur R, Mekhilef S, Mahian O. Progress and latest developments of evacuated tube solar collectors. *Renew Sustain Energy Rev.* 2015;51:1038–54.
 59. Mahian O, Kianifar A, Sahin AZ, Wongwises S. Entropy generation during Al_2O_3 /water nanofluid flow in a solar collector: effects of tube roughness, nanoparticle size, and different thermophysical models. *Int J Heat Mass Transf.* 2014;78:64–75.
 60. Dehaj MS, Mohiabadi MZ. Experimental study of water-based CuO nanofluid flow in heat pipe solar collector. *J Therm Anal Calorim.* 2019. <https://doi.org/10.1007/s10973-019-08046-6>.
 61. Mahian O, Kianifar A, Sahin AZ, Wongwises S. Performance analysis of a minichannel-based solar collector using different nanofluids. *Energy Convers Manag.* 2014;88:129–38.
 62. Mahian O, Kianifar A, Heris SZ, Wongwises S. First and second laws analysis of a minichannel-based solar collector using boehmite alumina nanofluids: effects of nanoparticle shape and tube materials. *Int J Heat Mass Transf.* 2014;78:1166–76.
 63. Mahian O, Kianifar A, Kalogirou SA, Pop I, Wongwises S. A review of the applications of nanofluids in solar energy. *Int J Heat Mass Transf.* 2013;57:582–94.
 64. Noie S. Heat transfer characteristics of a two-phase closed thermosyphon. *Appl Therm Eng.* 2005;25:495–506.
 65. Reay D, McGlen R, Kew P. *Heat pipes: theory, design and applications.* Butterworth-Heinemann; 2013.
 66. Mahfoud M, Emadi D. Application of heat pipe technology in thermal analysis of metals. *J Therm Anal Calorim.* 2005;81:161–7.
 67. Akbari A, Saidi MH. Experimental investigation of nanofluid stability on thermal performance and flow regimes in pulsating heat pipe. *J Therm Anal Calorim.* 2018. <https://doi.org/10.1007/s10973-018-7388-3>.
 68. Kamalgharibi M, Hormozi F, Zamzamin SAH, Sarafraz M. Experimental studies on the stability of CuO nanoparticles dispersed in different base fluids: influence of stirring, sonication and surface active agents. *Heat Mass Transf.* 2016;52:55–62.
 69. Salari E, Peyghambarzadeh SM, Sarafraz MM, Hormozi F. Boiling thermal performance of TiO_2 aqueous nanofluids as a coolant on a disc copper block. *Periodica Polytech, Chem Eng.* 2016;60:106–22.
 70. Sarafraz M, Hormozi F. Experimental study on the thermal performance and efficiency of a copper made thermosyphon heat pipe charged with alumina–glycol based nanofluids. *Powder Technol.* 2014;266:378–87.
 71. Sarafraz M, Hormozi F. Intensification of forced convection heat transfer using biological nanofluid in a double-pipe heat exchanger. *Exp Thermal Fluid Sci.* 2015;66:279–89.
 72. Sarafraz M, Hormozi F. Experimental investigation on the pool boiling heat transfer to aqueous multi-walled carbon nanotube nanofluids on the micro-finned surfaces. *Int J Therm Sci.* 2016;100:255–66.
 73. Sarafraz M, Hormozi F, Kamalgharibi M. Sedimentation and convective boiling heat transfer of CuO-water/ethylene glycol nanofluids. *Heat Mass Transf.* 2014;50:1237–49.
 74. Sarafraz M, Hormozi F, Nikkhah V. Thermal performance of a counter-current double pipe heat exchanger working with COOH-CNT/water nanofluids. *Exp Thermal Fluid Sci.* 2016;78:41–9.
 75. Sarafraz M, Peyghambarzadeh S, Hormozi F, Vaelim N. Experimental studies on the upward convective boiling flow to DI-water and CuO nanofluids inside the annulus. *J Appl Fluid Mech.* 2015;8(4):651–9.
 76. Sarafraz M, Hormozi F, Silakhori M, Peyghambarzadeh S. On the fouling formation of functionalized and non-functionalized carbon nanotube nano-fluids under pool boiling condition. *Appl Therm Eng.* 2016;95:433–44.
 77. Sarafraz M, Nikkhah V, Nakhjavani M, Arya A. Fouling formation and thermal performance of aqueous carbon nanotube nanofluid in a heat sink with rectangular parallel microchannel. *Appl Therm Eng.* 2017;123:29–39.
 78. Sarafraz M, Peyghambarzadeh S. Experimental study on sub-cooled flow boiling heat transfer to water–diethylene glycol mixtures as a coolant inside a vertical annulus. *Exp Therm Fluid Sci.* 2013;50:154–62.
 79. Sarafraz M, Peyghambarzadeh S, Alavifazel S. Enhancement of nucleate pool boiling heat transfer to dilute binary mixtures using endothermic chemical reactions around the smoothed horizontal cylinder. *Heat Mass Transf.* 2012;48:1755–65.
 80. Sarafraz MM, Hormozi F. Forced convective and nucleate flow boiling heat transfer to alumina nanofluids. *Periodica Polytech, Chem Eng.* 2014;58:37–46.
 81. Sarafraz S, Peyghambarzadeh M, Vaeli N. Subcooled flow boiling heat transfer of ethanol aqueous solutions in vertical annulus space. *Chem Ind Chem Eng Quart/CICEQ.* 2012;18: 315–27.
 82. Sajid MU, Ali HM, Sufyan A, Rashid D, Zahid SU, Rehman WU. Experimental investigation of TiO_2 –water nanofluid flow and heat transfer inside wavy mini-channel heat sinks. *J Therm Anal Calorim.* 2019. <https://doi.org/10.1007/s10973-019-08043-9>.
 83. Shah TR, Ali HM. Applications of hybrid nanofluids in solar energy, practical limitations and challenges: a critical review. *Sol Energy.* 2019;183:173–203.
 84. Sajid MU, Ali HM. Thermal conductivity of hybrid nanofluids: a critical review. *Int J Heat Mass Transf.* 2018;126:211–34.
 85. Toghyani S, Afshari E, Baniyasi E, Shadloo MS. Energy and exergy analyses of a nanofluid based solar cooling and hydrogen production combined system. *Renew Energy.* 2019;141:1013–25.
 86. Dehaj MS, Mohiabadi MZ. Experimental investigation of heat pipe solar collector using MgO nanofluids. *Sol Energy Mater Sol Cells.* 2019;191:91–9.
 87. Xu R, Zhang C, Chen H, Wu Q, Wang R. Heat transfer performance of pulsating heat pipe with zeotropic immiscible binary mixtures. *Int J Heat Mass Transf.* 2019;137:31–41.

88. Zhang S, Chen J, Sun Y, Li J, Zeng J, Yuan W, Tang Y. Experimental study on the thermal performance of a novel ultra-thin aluminum flat heat pipe. *Renew Energy*. 2019;135:1133–43.
89. Sarafraz M, Hormozi F, Peyghambarzadeh S. Role of nanofluid fouling on thermal performance of a thermosyphon: are nanofluids reliable working fluid? *Appl Therm Eng*. 2015;82:212–24.
90. Wei A, Qu J, Qiu H, Wang C, Cao G. Heat transfer characteristics of plug-in oscillating heat pipe with binary-fluid mixtures for electric vehicle battery thermal management. *Int J Heat Mass Transf*. 2019;135:746–60.
91. Alavi Fazel S, Sarafraz M, Arabi Shamsabadi A, Peyghambarzadeh S. Pool boiling heat transfer in diluted water. *Heat Transf Eng*. 2013;34:828–37.
92. Arya A, Shahmiry S, Nikkhah V, Sarafraz MM. Cooling of high heat flux flat surface with nanofluid assisted convective loop: experimental assessment. *Arch Mech Eng*. 2017;64:519–31.
93. Fazel SA, Sarafraz M, Shamsabadi AA, Peyghambarzadeh S. Pool boiling heat transfer in diluted water/glycerol binary solutions. *Heat Transf Eng*. 2013;34:828–37.
94. Fazel SA, Shamsabadi AA, Sarafraz M, Peyghambarzadeh S. Artificial boiling heat transfer in the free convection to carbonic acid solution. *Exp Therm Fluid Sci*. 2011;35:645–52.
95. Peyghambarzadeh S, Sarafraz M, Vaeli N, Ameri E, Vatani A, Jamialahmadi M. Forced convective and subcooled flow boiling heat transfer to pure water and *n*-heptane in an annular heat exchanger. *Ann Nucl Energy*. 2013;53:401–10.
96. Sarafraz M, Arya H, Saeedi M, Ahmadi D. Flow boiling heat transfer to MgO-therminol 66 heat transfer fluid: experimental assessment and correlation development. *Appl Therm Eng*. 2018;138:552–62.
97. Sarafraz M, Fazel AS, Hasanzadeh Y, Arabshamsabadi A, Bahram S. Development of a new correlation for estimating pool boiling heat transfer coefficient of MEG/DEG/water ternary mixture. *Chem Ind Chem Eng Quart/CICEQ*. 2012;18:11–8.
98. Sarafraz M, Hormozi F. Application of thermodynamic models to estimating the convective flow boiling heat transfer coefficient of mixtures. *Exp Therm Fluid Sci*. 2014;53:70–85.
99. Sarafraz MM, Peyghambarzadeh S, Alavi FS. Experimental studies on nucleate pool boiling heat transfer to ethanol/MEG/DEG ternary mixture as a new coolant. *Chem Ind Chem Eng Quart/CICEQ*. 2012;18:577–86.
100. Tsai C, Chien H, Ding P, Chan B, Luh T, Chen P. Effect of structural character of gold nanoparticles in nanofluid on heat pipe thermal performance. *Mater Lett*. 2004;58:1461–5.
101. Moffat RJ. Describing the uncertainties in experimental results. *Exp Therm Fluid Sci*. 1988;1:3–17.
102. Sarafraz M, Pourmehran O, Yang B, Arjomandi M. Assessment of the thermal performance of a thermosyphon heat pipe using zirconia-acetone nanofluids. *Renew Energy*. 2019;136:884–95.
103. Sarafraz M, Hormozi F, Peyghambarzadeh S. Thermal performance and efficiency of a thermosyphon heat pipe working with a biologically ecofriendly nanofluid. *Int Commun Heat Mass Transfer*. 2014;57:297–303.

Publisher's Note Springer Nature remains neutral with regard to jurisdictional claims in published maps and institutional affiliations.